Scientific Research Publishing

American Journal of Climate Change, 2022, 11, 197-229
https://www.scirp.org/journal/ajcc
ISSN Online: 2167-9509
ISSN Print: 2167-9495

The Influence and Implications of Climate Change on Water Quality in a Large Water Reservoir in the Southwest, USA

Deena Hannoun*, Todd Tietjen, Keely Brooks

Southern Nevada Water Authority, Henderson, NV, USA
Email: *deena.hannoun@snwa.com

How to cite this paper: Hannoun, D., Tietjen, T. and Brooks, K. (2022). The Influence and Implications of Climate Change on Water Quality in a Large Water Reservoir in the Southwest, USA *American Journal of Climate Change, 11,* 197-229.
https://doi.org/10.4236/ajcc.2022.113010

Received: May 12, 2022
Accepted: September 25, 2022
Published: September 28, 2022

Copyright © 2022 by author(s) and Scientific Research Publishing Inc.
This work is licensed under the Creative Commons Attribution International License (CC BY 4.0).
http://creativecommons.org/licenses/by/4.0/

Open Access

Abstract

Maintaining water quality in large reservoirs is crucial to ensure continued delivery of high-quality water to consumers for municipal and agricultural needs. Lake Mead, a large reservoir in the desert southwest, USA, is projected to be affected by both loss of volume and rising air temperatures through the end of the 21st century. In this study, reductions in lake volume, coupled with downscaled climate projections for rising air temperatures through the end of the 21st century, are incorporated into the 3D hydrodynamic and water quality model for Lake Mead. If current management practices continue in the future, simulations indicate water temperatures will increase in all scenarios and could increase by as much 2˚C under the most pessimistic scenarios, but nutrient loads would not increase to concerning levels. Releases from the dam to downstream users are projected to be much warmer, and warmer water temperatures and significant dissolved oxygen in the water column are expected to cause challenges for ecosystem and recreation in the future. Surprisingly, during the Winter and Autumn, retention of heat in Lake Mead is more pronounced at higher surface elevations than the lower elevations as expected. The effects of these projections on the lake water quality and consequently, lake management decisions, are discussed.

Keywords

Climate Change, Lake Management, Water Quality Modeling, Lake Mead, AEM3D

1. Introduction

Reservoirs are important sources of drinking water, and they, like other bodies of water, are being impacted by decline in water quality due to climate change

(Sahoo et al., 2016). One study estimates that lake surface water temperatures have increased worldwide at a global average rate of 0.34˚C per decade, which is similar to or in excess of air temperature trends (Woolway, Kraemer, Lenters, O'Reilly, & Sharma, 2020). This warming can reduce water quality by altering thermal stratification patterns and nutrient cycling, and therefore is an important consideration for water managers. Unlike natural lakes, reservoirs respond differently to climate change because storage and outflow are actively managed, and this can result in unexpected changes to water quality and reservoir stratification (Butcher, Nover, Johnson, & Clark, 2015).

While several studies have projected the effects of climate change, specifically warming of ambient air temperature and inflows, on lakes and reservoirs across a broad national or global scale, the effects of climate change on the management of large, arid-region reservoirs are not currently well-understood. Specifically, this study seeks to answer how increasing air temperatures and reductions in reservoir volume may affect water quality in systems where inflow and outflow are highly-managed. Here, an actively managed large reservoir in the desert southwestern United States, Lake Mead, is evaluated and the response of water quality at various lake elevations is tested against future air temperature warming projected from climate models.

Three-dimensional modeling of lakes and reservoirs using Aquatic Ecosystem Model 3D (AEM3D; formerly ELCOM/CAEDYM), to project water quality parameters such as water temperature, dissolved oxygen (DO), and nutrients, is a long-standing practice to understand how lakes and reservoirs may be affected by changes to the ecosphere (Allan, Hamilton, & Muraoka, 2017; Amadori et al., 2021; Chung, Hipsey, & Imberger, 2009; Chung, Imberger, Hipsey, & Lee, 2014; Gao, He, Fang, Bai, & Huang, 2018; Hannoun, Tietjen, & Brooks, 2021; Preston, Hannoun, List, Rackley, & Tietjen, 2014; Saber, James, & Hannoun, 2020; Zamani, Koch, & Hodges, 2020).

The Southern Nevada Water Authority (SNWA) maintains a three-dimensional hydrodynamic and water quality model, implemented in AEM3D, for Lake Mead that is used to simulate probable future scenarios and to aid in management decisions and facilities planning. The model has been verified and validated, and has been used historically as a decision support tool, including determining optimal placement of a newly constructed drinking water intake (Preston, Hannoun, List, Rackley, & Tietjen, 2014) and for projecting how source water quality and water treatment processes may change (Hannoun, Tietjen, & Brooks, 2021).

In this study, the model is used to project how in-situ lake parameters, including water temperature, DO, phosphorus, and nitrogen, may change as a result of loss of volume and rising air temperatures applied to Lake Mead. Water temperature and DO are important parameters that potentially impact aquatic life in the lake. Higher water temperatures and reduced DO could have negative impacts on aquatic life. Phosphorus, a common constituent in agricultural runoff and wastewater, can negatively speed up eutrophication of lakes and con-

tribute to algal blooms at high levels (Horne & Goldman, 1994). Similar to phosphorus, an overabundance of nitrogen can contribute to overstimulation of growth of aquatic plants and algae. Further, warmer water coupled with higher concentrations of nitrogen and phosphorus leads to the potential for algal blooms in Lake Mead (Hannoun, Tietjen, & Brooks, 2021). While the effects of projected rising air temperatures and extreme loss of lake volume are now better understood for one modeled cell of Lake Mead through which water is withdrawn for treatment and distribution (Hannoun, Tietjen, & Brooks, 2021), the effects of these drivers are not well-understood for the whole lake. In this study, the effects of projected rising air temperature and extreme loss of lake volume on water quality parameters in the most downstream basin of Lake Mead are studied. This study is novel as it provides suggestions for continued strategies to ensure maintenance of water quality for arid, highly-managed systems that are stressed by rising air temperatures and loss of volume.

2. Materials and Methods

2.1. Study Area

Lake Mead (**Figure 1**), a large reservoir in the desert southwestern United States, is crucial as a link in the highly-controlled Lower Colorado River Basin that provides drinking and irrigation water for over 40 million people (Colorado River Water Users Association, 2021; Milly & Dunne, 2020). Being in a hot and arid region that rarely experiences below freezing air temperature, Lake Mead never experiences ice cover like temperate region lakes, only cooling to 10˚C - 12˚C each winter. These thermal patterns are similar to downstream Lakes Mohave and Havasu, but significantly warmer than reservoirs in non-arid climates (Southern Nevada Water Authority, 2021).

Stratification in lakes and reservoirs is a process where solar radiation and warmer ambient air temperature applied to the surface of the lake create a depth-sensitive water temperature gradient (Casamitjana, Serra, Colomer, Beserba, & Perez-Losada, 2003). In the northern hemisphere, this phenomenon typically occurs during summer and can persist into Autumn. In the winter, the lake will begin to mix top to bottom and the magnitude of the thermal gradient will either become nonexistent (if the lake fully mixes) or very small (if the lake does not mix entirely). Stratification patterns in Lake Mead show strong thermal stratification in summer with the top of the water column reaching 27˚C and the lake mixing fully during winter approximately half of the years. During the years that the lake does not mix fully, there is weak thermal stratification through winter and early Spring (Preston, Hannoun, List, Rackley, & Tietjen, 2014).

While 97% of inflow into the reservoir is from the Colorado River from the east, 0.7% of inflow comes from the Las Vegas Wash (the Wash, green arrow, **Figure 1**) into Boulder Basin (yellow circle, **Figure 1**). The remaining inflow into Lake Mead is from the Virgin and Muddy Rivers (from the North). The inflowing Colorado River is historically lower in temperature than the ambient

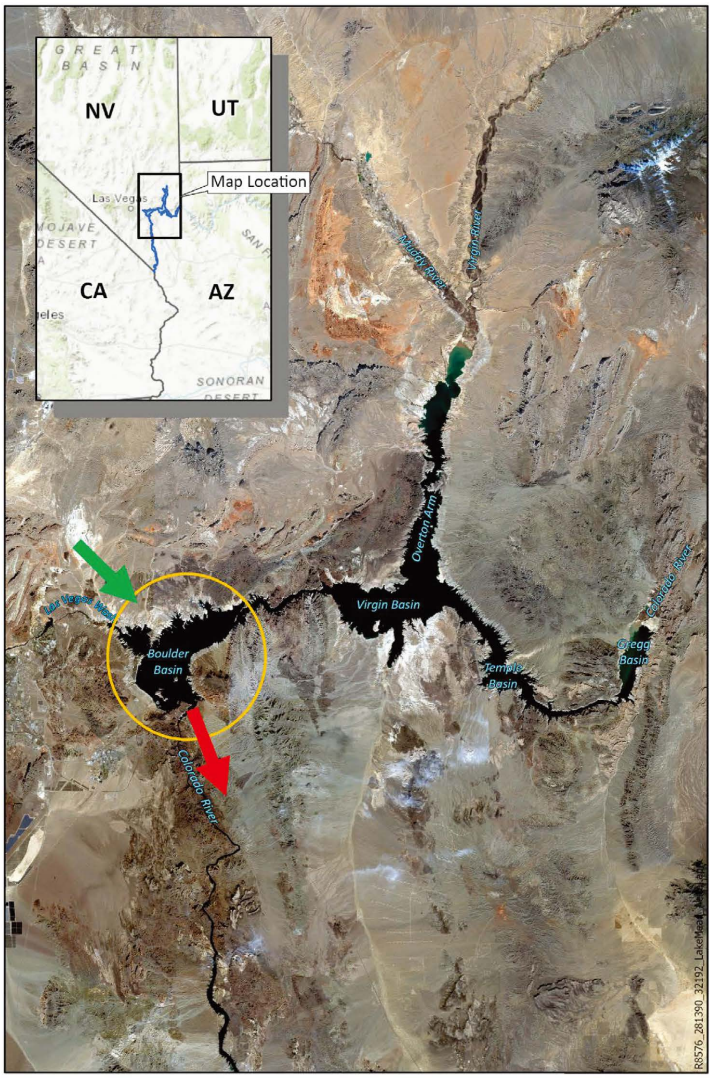

Figure 1. Lake Mead Map. Las Vegas Wash inflow into Boulder Basin is circled in yellow. Outflow is through the Colorado River south out of Boulder Basin (red arrows). Las Vegas Wash influent is highlighted by the green arrow.

Lake Mead water and enters as an underflow (Preston, Hannoun, List, Rackley, & Tietjen, 2014). The Colorado River water is relatively high-quality, as it is low in temperature and limited in phosphorus; however, it has a moderate nitrogen and organic content, thus making the susceptible to harmful algal blooms. This means that Lake Mead's inflow is dominated by high-quality water capable of diluting constituents from the more anthropogenically impacted Las Vegas Wash.

The inflow from the Wash into Lake Mead is important because it comprises the majority of the nutrient load for Boulder Basin (Ding, Hannoun, List, & Tietjen, 2014). The Wash is comprised of approximately 90% highly treated wastewater from the Las Vegas Valley. Wastewater discharge into the Wash is highly regulated with strict nutrient limits, including total maximum daily loads

(TMDLs) for phosphorus and ammonia to maintain low chlorophyll a concentration. There is also a requirement to maintain higher water quality (RMHQ) for nitrogen (Nevada Division of Environmental Protection, 2003). One concern is that warming waters from climate change and lake drawdown could result in an increase in harmful algal blooms, or an increase in anoxic conditions. Most outflow from Lake Mead is released downstream through the Hoover Dam (red arrow, **Figure 1**), which is located on the southern tip of Boulder Basin, with minor diversions from SNWA's drinking water intake (Intake 3) and losses from evapotranspiration (Preston, Hannoun, List, Rackley, & Tietjen, 2014).

Maintaining the high water quality of Lake Mead is crucial to the Lower Colorado River Basin; however, the lake has already experienced a significant decrease in volume due to prolonged drought and aridification (United States Bureau of Reclamation, 2020b). SNWA draws raw drinking water from Lake Mead for treatment and distribution to the Las Vegas Valley's 2.2 million residents and 43 million annual tourists. Drinking water Intakes 1 and 2 are no longer used due to their proximity to the surface of the lake, leading to the potential for warmer, epilimnetic withdrawals in the summer. Further, the Hoover Dam Upper Outlet is currently below the water surface; therefore, releases are only being made through the Lower Outlet (**Table 1**). Currently, drinking water for the Las Vegas Valley is withdrawn through Intake 3, which will have an operational capacity beyond the point that Hoover Dam is no longer able to release water downstream (**Figure 2**; **Table 1**). Climate change has already changed some operations in Lake Mead, and in the future, it may have critical effects on Lake Mead, including changes to water quality parameters as a result of lake drawdown and rising air temperatures (Udall & Overpeck, 2017). Boulder Basin of Lake Mead is selected for this study as it is the most downstream basin of Lake Mead (**Figure 1**, yellow circle) and consequently absorbs the effects of all tributaries and contains both SNWA's drinking water intake and the Hoover Dam.

Table 1. Important elevations for Lake Mead (Southern Nevada Water Authority, 2022; United States Bureau of Reclamation, 2008).

Lake Characteristic/Infrastructure	Elevation (m (ft) above sea level)
Full pool	372 (1220)
Current Lake Mead Elevation	321 (1043)
Hoover Dam Upper Outlet	319 (1045)
Withdrawal elevation for Intakes 1 & 2*	302 (992)
Hoover Dam Lower Outlet**	273 (895)
Withdrawal elevation for Intake 3	273 (895)
Operational threshold for Intake 3	262 (860)

*No longer used. **Lowest water outlet, below this elevation is dead storage where water cannot be released downstream given current options.

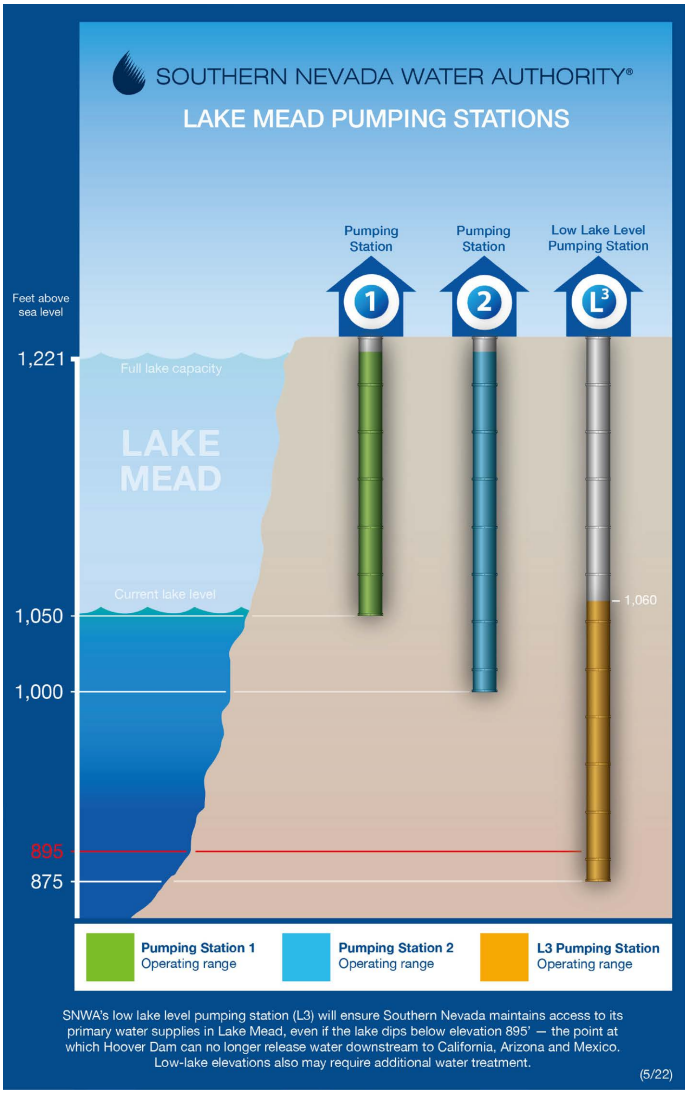

Figure 2. SNWA's Intake withdrawal depths.

2.2. Lake Mead Model Inputs

SNWA maintains a 3D hydrodynamic and water quality model for Lake Mead to simulate water quality under projected future scenarios, including drawdown, climate change, and projected future flow scenarios, called the Lake Mead Model (LMM). The LMM is implemented in AEM3D, which approximates quantities of interest by solving the Reynolds-averaged Navier-Stokes equations with a turbulent eddy closure and wind-forced mixing model (Hodges & Dallimore, 2019). The model solves for hydrodynamic parameters, including water temperature, salinity, and DO, and nutrients, such as nitrogen, phosphorus, and carbon. The LMM grid is based on lake bathymetry and uses a 300 × 300 meter x-y grid with depth outputs every 2 meters. Inflow data from the Colorado River is measured by the United States Geological Survey (USGS) monitoring gauge located at Diamond Creek near Peach Springs, AZ, upriver from Lake Mead. This gauge also monitors other forcing parameters, such as water temperature, DO,

pH, and suspended sediment (USGS, 2020a). Inflow volumes from the Virgin and Muddy Rivers are determined from USGS gauges located at Littlefield, AZ (USGS, 2020d) and Moapa, NV (USGS, 2020c), respectively. Additional water quality parameters, including water temperature, DO, conductivity, and pH are collected by deployed Hydrolab HL4 sondes near each of these sites, which take readings every 15 minutes. Inflow rates at the Wash are measured by a USGS gauge located at Pabco Road, Henderson, NV (USGS, 2020b). Additional parameters, including water temperature, DO, conductivity, and pH, are again monitored by a deployed Hydrolab HL4 sonde near the Pabco Road gauge. Outflow volumes for Hoover Dam and the SNWA drinking water intake are provided by the Bureau of Reclamation (United States Bureau of Reclamation, 2020a). Nutrient parameters such as nitrogen and phosphorus that are input in the model are collected as part of inter-agency sampling efforts in the Las Vegas Valley and are published in the Lower Colorado Water Quality Database (Southern Nevada Water Authority, 2021).

Meteorological parameters are input into the model as boundary forcing values. Rainfall data is measured by the National Oceanic and Atmospheric Administration (NOAA) at Harry Reid International airport, approximately 48 kilometers (30 miles) away from Lake Mead. Total rainfall is assumed to be uniform in the simulated region; however, it is an almost negligent contribution to the lake elevation and is typically around four inches per year (NOAA, 2019). Wind speed and direction are taken from the NOAA weather buoys deployed in Lake Mead. Solar radiation is measured by the National Renewable Energy Laboratory instruments at the University of Nevada, Las Vegas, approximately 50 kilometers (31 miles) from the lake (NREL, 2020). Cloud cover is assumed to be zero as pyrometer data has not been evaluated and there is typically little cloud cover in southern Nevada (NOAA, 2022).

2.3. Model Calibration

The LMM was calibrated to measured field data to ensure model accuracy and minimization of error as a future planning tool. First, a sensitivity analysis was conducted in MATLAB to determine which parameters are most sensitive to numerical perturbations. A wrapper around the AEM3D code perturbed selected parameters and change in model output was measured and normalized by the perturbation, such that

$$\frac{f(x+h)-f(x)}{h}. \tag{1}$$

In Equation (1), f is the AEM3D output, x is the variable for which we are measuring the perturbation, and h is the perturbation. Sensitivity analysis calculates a derivative that is used to determine which input parameters are most sensitive to small changes (Saltelli, Tarantola, & Campolongo, 2000).

Through sensitivity analysis, three model parameters were determined to be most affected by perturbations: the wind shear coefficient, the mean albedo, and

the surface heat transfer coefficient. The wind shear coefficient, represented in the model by $wind_{cd}$, is used as a multiplier to calculate the wind shear velocity from the calculated wind velocity. It appears in the model as

$$u_* = \sqrt{wind_{cd} \frac{\rho_{air}}{\rho_0}} U_{wind}, \tag{2}$$

where u_* is the wind shear velocity, ρ_{air} and ρ_0 are the density of air and fresh water, respectively, and U_{wind} is the wind velocity as calculated by the model. Ultimately, $wind_{cd}$ controls how much wind shear is put into the model and consequently affects mixing and water temperature.

Another parameter found to be significant by sensitivity analysis is mean albedo. This is represented in the model by *r*, is the reflection coefficient of both short and long wave radiation and varies from lake to lake depending on lake color, wave state, and angle of the sun (Hodges & Dallimore, 2013). The albedo appears in the model in two instances, including (Tennessee Valley Authority, 1972)

$$Q_{sw} = Q_{sw(total)}(1-r) \quad \text{and} \tag{3}$$

$$Q_{lw(rad)} = Q_{lw(air)}(1-r). \tag{4}$$

Equation (3) accounts for the shortwave radiation that penetrates the lake surface and Equation (4) accounts for the longwave radiation that penetrates the lake surface. Albedo ultimately determines how much radiation is absorbed by the lake. The surface heat transfer coefficient, represented in the model by C_s, is the final parameter identified by the sensitivity analysis to have a large effect on the model output. C_s is used to calculate the sensible heat loss Q_{sh} at the surface of the lake over the time period Δt, given by

$$Q_{sh} = C_s \rho_a C_p U_a (T_a - T_s) \Delta t. \tag{5}$$

Here, ρ_a is the density of the air, U_a is the wind velocity, and T_a and T_s are the air and water temperature, respectively (Saber, James, & Hannoun, 2020).

Once sensitive parameters were identified, a nonlinear least squares algorithm was used to identify optimal parameter values that minimize the residual between model output and collected field data. Again, a wrapper around the AEM3D code was written in MATLAB to determine these optimal values. The MATLAB nonlinear least squares solver *lsqnonlin*, which is a Levenberg-Marquardt algorithm, was used (MathWorks, 2021).

Optimal values for the parameters were found to be

$$wind_{cd} = 1.72 \times 10^{-3}, \tag{6}$$

$$r = 0.22, \text{ and} \tag{7}$$

$$C_s = 1.8 \times 10^{-3}. \tag{8}$$

Once optimal values were determined, the model was re-run with optimal values to investigate the residuals for transported scalars over space and time (Section 3.1).

2.4. Climate Change Projections

Climate change projections for Clark County, NV, which encompasses the Las Vegas Valley and the portion of Lake Mead in Nevada, were incorporated into the LMM to determine how future probable climate scenarios may affect water quality in a large, managed reservoir. Maximum daily air temperatures for Clark County, NV were output from six Global Climate Models (GCMs) and downscaled using the Localized Constructed Analogs (LOCA) technique (Pierce, Cayan, & Thrasher, 2014). This was done for two climate change scenarios, Representative Concentration Pathway 4.5 and 8.5 (RCP 4.5 and RCP 8.5). RCPs represent potential future atmospheric concentrations of greenhouse gases (GHGs) and reflect the amount of radiative forcing that would result. RCP 8.5 uses 8.5 W/m^2 and RCP 4.5 uses 4.5 W/m^2 (Kalansky, Sheffield, Cayan, & Pierce, 2018; Kim, Lee, Park, & Kil, 2015). RCP 8.5 assumes emissions continue to be emitted at the current rate and above, whereas RCP 4.5 is more conservative and assumes a reduction in emissions due to comprehensive global GHG mitigation (Kalansky, Sheffield, Cayan, & Pierce, 2018). Consistent with literature regarding climate change, RCP 8.5 typically produces more pessimistic (i.e. warmer) results (Chao et al., 2014).

Consistent with the RCPs, air temperature projections for Clark County for three periods, 2010-2039 (near-term), 2040-2069 (mid-century), and 2070-2099 (late-century) were incorporated into the LMM by altering meteorological forcing functions (Kalansky, Sheffield, Cayan, & Pierce, 2018). The forcing functions were updated to reflect the average projected increase in air temperature for each year. Further, these air temperature changes were coupled with changes in lake elevation due to drawdown. Testing how these changes impact the LMM allow water managers to anticipate possible future water quality conditions based on climate change, and proactively develop strategies to adapt to the impacts of climate change on water quality.

2.5. LMM Simulations

In totality, 35 model runs were performed, which yield a wide array of possible future scenarios (Supplemental Materials; **Table S1**). Five potential starting water surface elevation levels (WSELs) were investigated: 335, 320, 305, 290, and 274 meters (1100, 1050, 1000, 950, and 900 feet). Lake Mead is at full pool at 372 meters (1220 feet) and dead storage at 273 meters (895 feet). The selected WSELs represent a wide range of possible scenarios. Higher WSELs were not considered as the lake is currently at an elevation of 321 meters (1054 feet). Next, three clusters of years were evaluated, 2010-2039 (near-term), 2040-2069 (mid-century), and 2070-2099 (late-century), consistent with methods from similar studies (Chao et al., 2014; Kalansky, Sheffield, Cayan, & Pierce, 2018). Then, two climate scenarios were simulated, RCP 4.5 and RCP 8.5. Finally, a climate normal baseline simulation which assumes historical meteorological conditions for the early 2000s was performed at each of the five WSELs as a basis for comparison to the

effects of climate change input into the LMM. Simulated parameters in this study include water temperature, total inorganic nitrogen (TIN), total phosphorus (TP), and DO. A one-year burn-in period is included to allow equilibrium away from initial conditions. A flow chart showing the modeling framework for this study shows model inputs that were modified (Figure 3; green arrows), model inputs taken from historic data (Figure 3; blue arrow), and model outputs (Figure 3; purple arrows).

2.6. Analysis of LMM Simulations

The LMM solves for quantities of interest, in this case, water temperature, DO, nitrogen, and phosphorus, over the entirety of Lake Mead, which includes over 200,00 grid cells at each time step. Results presented in this study are downscaled and postprocessed from the raw model output.

Analyses of model runs were evaluated on both a seasonal and annual basis to look for trends in water quality parameters. For brevity, only results for the baseline scenario and most pessimistic (late-century/RCP 8.5) scenario are presented in the main text of this manuscript. The goal of this is to show a comparison between historic conditions and a worst-case climate scenario, as the RCP 8.5/late-century projections produce the most warming not only in the air temperature but also in the lake. Results are presented at each of the five simulated WSELs—335, 320, 305, 290, and 274 meters (1100, 1050, 1000, 950, and 900 feet). Additional results for all scenarios and time periods are available in the supplemental materials.

Seasonal mean maximum and minimum water temperatures serve as a signal to show how loss of volume in large reservoirs coupled with rising air temperatures may affect large, managed reservoirs over time. Boulder Basin of Lake Mead is selected for this study as it is the most downstream basin of Lake Mead (Figure 1, yellow circle) and consequently absorbs the effects of all tributaries and contains both SNWA's drinking water intake and the Hoover Dam (Section 3.2).

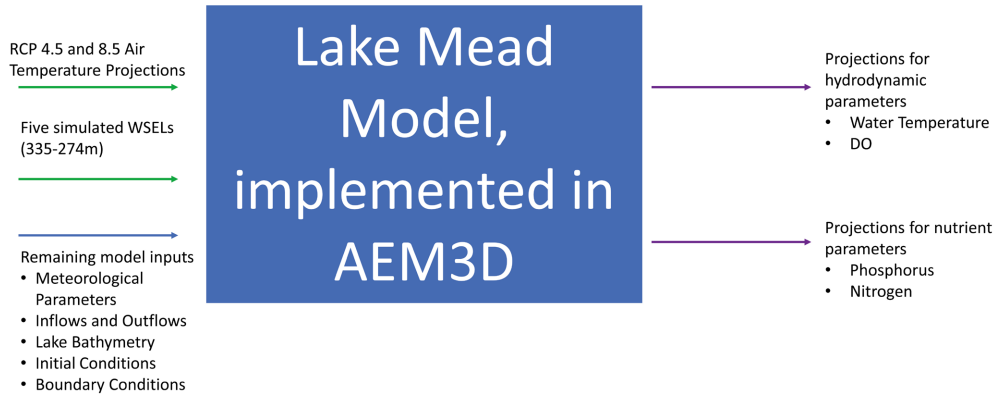

Figure 3. LMM modeling workflow. The green arrows indicate input quantities that were altered to evaluate model output (WSEL and air temperature projections), the blue arrows indicate historic inputs, and the purple arrows indicate model projections.

Annual trends for selected water quality parameters were investigated at different locations. Water temperature and DO trends were studied at several representative sites at the lake, including two sampling sites and the Hoover Dam. The two sampling sites—LVB 6.7, located in Las Vegas Bay, which was once 11 kilometers (6.7 miles) from the confluence of Boulder Basin and the Las Vegas Wash when Lake Mead was at full pool but is now approximately 5 kilometers (3 miles) from the confluence, and CR 346.4, located in deep water in Boulder Basin—were studied. For nutrient parameters, sites close to the Las Vegas Wash (i.e. LWLVB 1.2), which provides the majority of the nutrient load to Boulder Basin, were investigated. LWLVB 1.2 is a moving sampling site that is located 1.9 kilometers (1.2 miles) from the confluence of Boulder Basin and the Las Vegas Wash, regardless of lake elevation. The sampling site LWLVB 1.2 is a movable site located 1.9 kilometers (1.2 miles) from the current confluence of the Las Vegas Wash and Boulder Basin and has the highest potential for exceedances based on its proximity to the Wash (Section 3.3).

The Wilcoxon rank sum test (Gibbons & Chakraborti, 2011) was used to determine if the differences in the simulated parameters at each WSEL are statistically significantly different between the baseline and most pessimistic climate scenarios. An α of 0.01 was selected to test the null hypothesis that means are equal at each WSEL.

3. Results

3.1. Model Calibration

Thermocline plots coupled with field data collected by the City of Las Vegas using a YSI EXO sonde and residuals at different times of the year at sampling station CR 346.4, which is a deep site located in Inner Boulder Basin, show an excellent fit between the LMM and collected field data (**Figure 4**). These findings indicate an exceptional calibration of the model to available data, with root mean square errors (RMSEs) between 0.036˚C and 0.26˚C.

3.2. Seasonal Results: Water Temperature

Mean maximum and minimum water temperatures in winter (December, January, February) are crucial to maintaining water quality in Lake Mead. In 2001, a large algal bloom appeared in Boulder Basin. One driver behind this bloom was thought to be exceptionally warm winter water temperatures, approximately 1˚C - 2˚C greater than the historic mean (Southern Nevada Water Authority, 2021), preceding the summer bloom (Tietjen, 2015). Winter mean maximum and minimum water temperatures are projected to increase 1˚C - 2˚C from baseline at each of the five simulated WSELs when compared to the most pessimistic (RCP 8.5/late-century) climate scenario (**Table 2**). The greatest winter water temperature warming is projected to occur at higher lake elevations. This is because larger volumes of water retain residual heat from summer for longer periods of time (Horne & Goldman, 1994).

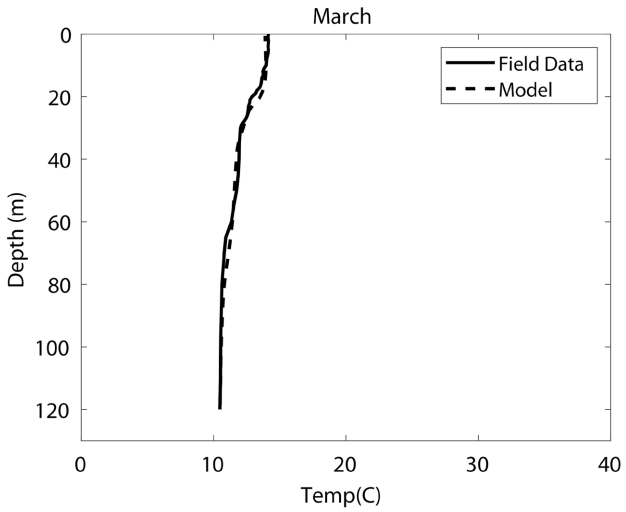

(a) March: RMSE = 3.6e-2˚C.

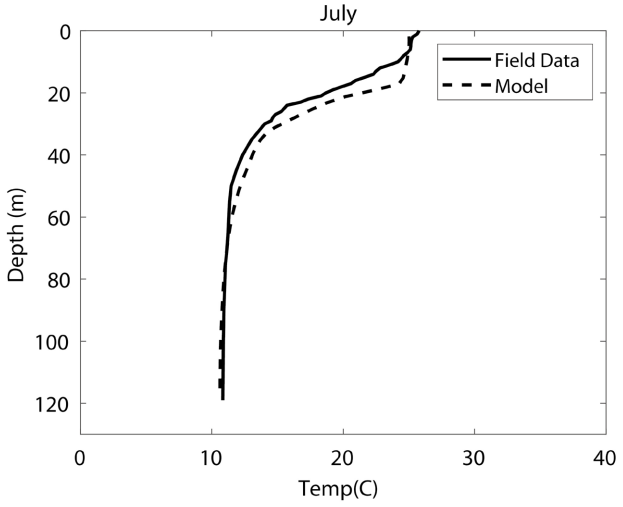

(b) July: RMSE = 2.6e-1˚C.

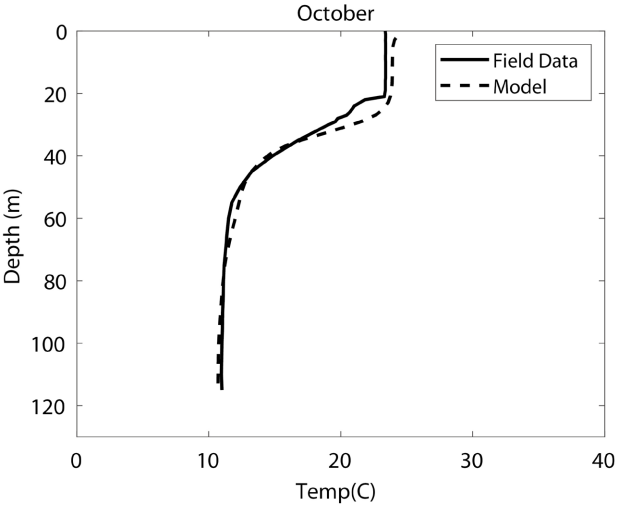

(c) October: RMSE = 1.5e-1˚C.

Figure 4. Model calibration results.

Table 2. Winter mean minimum and maximum temperatures: baseline scenario versus RCP 8.5/late century (most pessimistic) scenario.

	Winter Mean Maximum Water Temperature (˚C)		Winter Mean Minimum Water Temperature (˚C)	
Lake Elevations (m (ft) above sea level)	Baseline	RCP 8.5/late-century	Baseline	RCP 8.5/late-century
335 (1100)	15	17	13	15
320 (1050)	14	16	13	14
305 (1000)	13	15	12	13
290 (950)	13	15	12	13
274 (900)	13	15	12	13

Summer mean maximum water temperature trends are uniform across all five simulated WSELs. In the baseline scenario, mean maximum summer water temperatures are approximately 27˚C (Figure 5(a)). When increasing air temperatures are factored in the model in the most pessimistic scenario, the mean maximum summer water temperature increases to 29˚C (yellow bars, Figure 5(a)). Similar to summer, spring mean maximum water temperatures are projected to increase from 18˚C in the baseline scenario to approximately 20˚C in the most pessimistic scenario, regardless of simulated WSEL (purple bars, Figure 5(a)).

Autumn mean maximum water temperature trends are similar to winter, and are projected to increase as WSEL increases. A 1˚C - 2˚C mean maximum water temperature increase is projected at the two higher WSELs as there is more water volume present in the lake to retain heat.

Mean minimum water temperatures in Spring, Summer, and Autumn are also projected to increase in magnitude as the WSEL, and consequently lake volume, increases (Figure 5(b)).

Increasing air temperature from the baseline to the most pessimistic scenario also increases the mean maximum and minimum water temperatures at all five simulated WSELs (Figure 5).

3.3. Time Series Results

3.3.1. Water Temperature and Dissolved Oxygen

Water temperature and DO at three sites, LVB 6.7, CR 346.4, and the Hoover Dam, all within Boulder Basin, were investigated to look for differences attributed to projected climate change. Both water temperature and DO trends at Hoover Dam are important to be aware of potential changes in downstream releases to Lakes Mohave and Havasu, the next downstream reservoirs on the Colorado River. Water temperature and DO time series means along the vertical water column are reported at LVB 6.7 (Table 3) and CR346.4 (Table 4). At Hoover Dam (Table 5), mean water temperature and DO over time at the single modeled cell that contains the Lower Outlet are presented, as the Upper Outlet is not currently in use (Table 1).

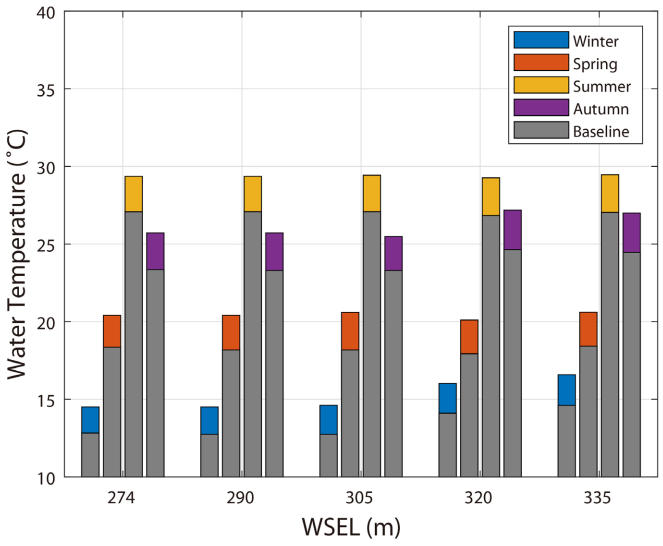

(a)

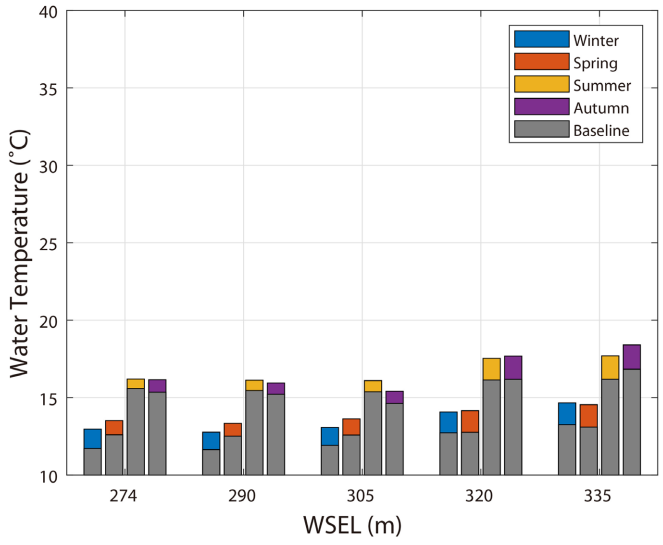

(b)

Figure 5. Mean maximum (a) top; and mean minimum (b) bottom; temperatures in Boulder Basin—most pessimistic scenario (colored bars) versus baseline scenario (gray bars).

Table 3. LVB 6.7 water temperatures and DO concentrations.

Lake WSELs (m (ft) above sea level)	Lake Volume (km^3)	Baseline Mean Temperature (˚C)	RCP 8.5/Late-Century Mean Temperature (˚C)	P-Value	Baseline Mean DO (mg/L)	RCP 8.5/Late-Century Mean DO (mg/L)	P-value
335 (1100)	14	18	19	<0.01	8.7	8.2	<0.01
320 (1050)	9.5	18	20	<0.01	8.7	8.2	<0.01
305 (1000)	5.5	19	21	<0.01	8.8	8.5	<0.01
290 (950)	2.5	20	22	<0.01	8.8	8.5	<0.01
274 (900)	0.21	20	22	<0.01	8.8	8.5	<0.01

Table 4. CR346.4 water temperatures and DO concentrations.

Lake WSELs (m (ft) above sea level)	Lake Volume (km^3)	Baseline Mean Temperature (˚C)	RCP 8.5/Late-Century Mean Temperature (˚C)	P-Value	Baseline Mean DO (mg/L)	RCP 8.5/Late-Century Mean DO (mg/L)	P-value
335 (1100)	14	15	17	<0.01	8.7	8.1	<0.01
320 (1050)	9.5	15	16	<0.01	8.8	8.2	<0.01
305 (1000)	5.5	14	15	<0.01	8.9	8.5	<0.01
290 (950)	2.5	15	16	<0.01	8.9	8.6	<0.01
274 (900)	0.21	15	16	<0.01	8.9	8.5	<0.01

Table 5. Hoover dam lower outlet water temperatures and DO concentrations.

Lake WSELs (m (ft) above sea level)	Lake Volume (km^3)	Baseline Mean Temperature (˚C)	RCP 8.5/Late-Century Mean Temperature (˚C)	P-Value	Baseline Mean DO (mg/L)	RCP 8.5/Late-Century Mean DO (mg/L)	P-value
335 (1100)	14	15	16	<0.01	8.8	8.3	<0.01
320 (1050)	9.5	17	18	<0.01	8.8	8.3	<0.01
305 (1000)	5.5	18	20	<0.01	8.9	8.5	<0.01
290 (950)	2.5	19	21	<0.01	8.9	8.5	<0.01
274 (900)	0.21	19	21	<0.01	8.9	8.5	<0.01

Yearly mean water temperatures at all three locations and all five WSELs are projected to increase by 1 - 2 degrees when the increase in air temperature from the most pessimistic climate scenario (RCP 8.5/late century) is factored into the model. All mean temperature differences are statistically significant. Warming as a result of loss of WSEL and volume is observed at LVB 6.7 and the Hoover Dam Lower Outlet (**Table 3** and **Table 5**); however, mean yearly lake temperatures are nearly consistent at the deeper site, CR 346.4, despite loss of WSEL and volume.

At all three sampling sites, stronger thermal stratification is projected in the summer (**Figure 6**; Supplemental Materials **Figure S1(a)**, **Figure S2(a)**, **Figure S3(a)**) from the baseline to most pessimistic climate scenario. Epilimnetic summer water temperatures are most susceptible to the highest magnitude of warming. There is also a small decrease in temperature at the bottom of the thermocline, which leads to a sharper temperature gradient in the most pessimistic climate scenario. Further, consistent with (Woolway et al., 2021), stratification begins earlier in the year and persists later in the year when climate effects are incorporated into the model (**Figure 6**).

At all three sampling sites, DO is projected to significantly decrease by 0.3 - 0.6 mg/L between the baseline and most pessimistic climate scenarios (**Tables 3-5**). At LVB 6.7 and the Hoover Dam Lower Outlet, there is a 0.1 mg/L increase in DO between the 320 and 305 meters (1050 and 1000 feet); however, these differences are not statistically significant (p-values of 0.053 and 0.061). At CR 346.4, the largest decrease in DO between the baseline and most pessimistic climate scenarios, 0.6 mg/L, is observed at the two highest WSELs, and is a function of a low DO water mixing in the lake at the beginning of the year in the most pessimistic scenario (Supplemental Materials **Figure S2(b)**).

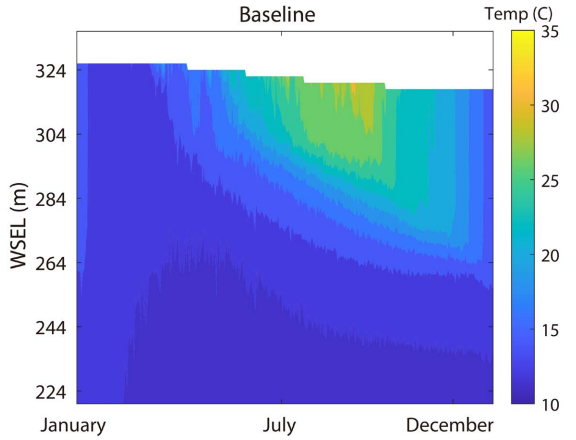

(a)

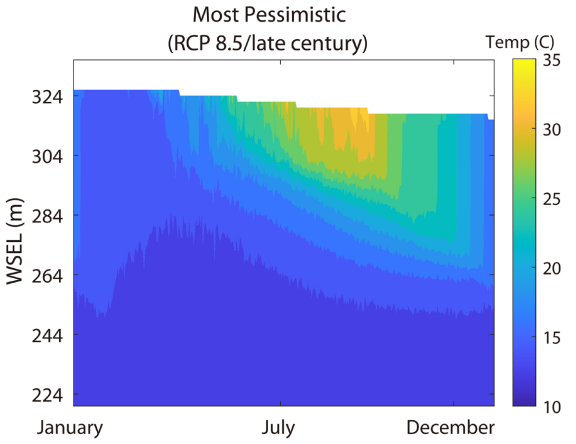

(b)

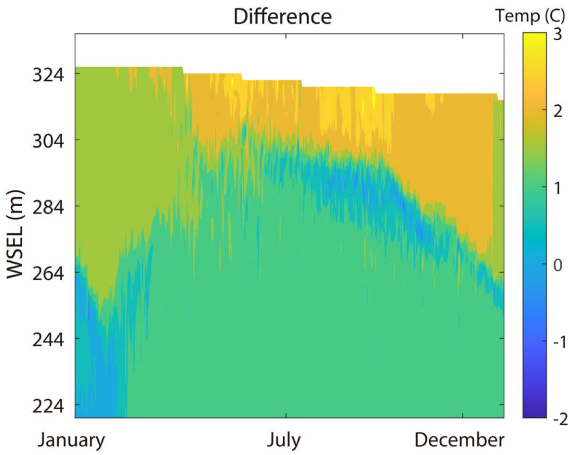

(c)

Figure 6. Water temperature contour plot; baseline (top); most pessimistic climate scenario (center); difference between the two thermoclines (bottom); stronger, prolonged stratification occurs in the most pessimistic scenario.

3.3.2. Total Phosphorus

Lake Mead is historically phosphorus-limited (LaBounty & Burns, 2005) and TP

levels do not change in any significant way in the modeled scenarios. This is largely due to the phosphorus removal protocols implemented by the four wastewater treatment facilities that discharge into the Las Vegas Wash. Predicted TP concentrations for all simulated scenarios at CR 346.4 ranged from 0 to 0.02 mg/L—extremely small values below model tolerance. Further, along the confluence of the Las Vegas Wash and Boulder Basin, where most nutrients enter the basin, TP maximum along the confluence is approximately 0.14 mg/L, regardless of WSEL or RCP/timeframe. This concentration will satisfy the TMDL for Lake Mead based on the Wash inflow rate (Nevada Division of Environmental Protection, 2003). These results indicate that phosphorus levels in Lake Mead will not be affected by loss of lake volume and climate change.

3.3.3. Total Inorganic Nitrogen

TIN is monitored in Boulder Basin in compliance with National Pollutant Discharge Elimination System (NPDES) permits. Compliance with this permit includes sampling for TIN in Boulder Basin so that discharging highly treated wastewater along the Las Vegas Wash into Lake Mead can continue.

Historically, measured deviations have occurred at the epilimnion, therefore, TIN values in the cells corresponding to the sampling sites were studied. The standard for LWLVB 1.2 is that 95% of TIN readings must be below 5.3 mg/L; the standard is 95% below 4.5 mg/L for the remainder of the lake (Nevada Division of Environmental Protection, 2003). Exceedances can have negative consequences, so it is important to use the model to be aware of the potential for such events in order to plan for mitigation of contaminants entering Lake Mead.

TIN concentration projections (mg/L) at LWLVB 1.2 were compared for the baseline and most pessimistic (RCP 8.5/late century) climate scenario at all five simulated WSELs (**Table 6**). At all five WSELs, there is no significant different between baseline and most pessimistic TIN concentrations. For WSELs of 335, 320, and 274 meters (1100, 1050, and 900 feet), no permit exceedances are projected for either climate scenarios. At 290 meters (950 feet), no exceedances are projected for the baseline scenario. Three exceedances could potentially occur in the most pessimistic scenario, but even considering this projection, 99.2% of TIN readings are below the 5.3 mg/L threshold, suggesting compliance. At 305 meters (1000 feet), the potential for exceedances in the second half of the year arise in both climate scenarios. In the baseline scenario, 65 TIN measurements greater than 5.3 mg/L may occur, yielding 82.2% of potential samples below the compliance limit. The most pessimistic climate scenario yields 33 potential exceedances, with 91.0% of samples below the compliance limit.

Predicted TIN at sampling site CR 346.4 remains low across all simulated scenarios, with maximum values ranging from 1.5 - 1.6 mg/L. This indicates that Colorado River-induced dilution in Boulder Basin dominates nutrient-rich inflow from the Las Vegas Wash in all considered probable future scenarios. Overall, TIN in Boulder Basin is not cause for concern under the simulated WSELs or climate scenarios.

Table 6. LWLVB 1.2 TIN concentrations.

Lake Elevations (m (ft) above sea level)	Baseline Mean TIN (mg/L)	RCP 8.5/Late-Century Mean TIN (mg/L)	P-Value	Baseline Percent of TIN Samples < 5.3 mg/L	RCP 8.5/Late-Century Percent of TIN Samples < 5.3 mg/L
335 (1100)	2.7	2.6	>0.01	100	100
320 (1050)	2.8	3.0	>0.01	100	100
305 (1000)	3.5	3.3	>0.01	**82**	**91**
290 (950)	2.9	3.0	>0.01	100	99
274 (900)	2.6	2.6	>0.01	100	100

3.4. Discussion

3.4.1. Seasonal Results

Seasonal temperature results yield several important observations. First, while winter mean maximum and minimum water temperatures are projected to increase with rising air temperatures, loss of volume in the lake yields cooler winter water temperatures. Thus, the three lower WSELs (305 meters (1000 feet) and below) could potentially prevent algal blooms from forming in Lake Mead, even in the face of the most pessimistic RCP 8.5/late-century climate scenario (Table 2; Figure 5).

A higher WSEL coupled with the most pessimistic climate scenario could lead to significant increases in mean winter water temperatures, leading to the potential for prolonged algal growth. This phenomenon of rising mean temperatures corresponding to larger water volumes also persists for the mean maximum temperature in Autumn as well as the year-round projected mean minimum temperature. This yields the unexpected finding that drawdown of large, managed systems, that are phosphorus and nitrogen limited may be beneficial when considering water temperatures and the potential for harmful algal blooms (HABs) alone when occurring in this narrow range.

Overall, increasing air temperatures have a larger effect on ambient lake water temperature when the WSEL is higher. These results indicate that projected rising air temperatures coupled with higher lake volumes have the potential to lead to the largest changes in temperature in Lake Mead. While lower WSELs may have positive impacts to prevent eutrophication in Boulder Basin as a whole, drawdown will also have negative impacts in Lake Mead, including Intake 3 withdrawing water from the deepening epilimnion in the summer months and withdrawing warmer water, which is projected to require additional treatment to meet delivery needs (Hannoun, Tietjen, & Brooks, 2021). Further, water released to downstream users will also be drawn from closer to the water surface, resulting in warmer releases to downstream users. This may impact not only downstream water quality, but also native aquatic life that is endangered and sensitive to change, such as the bonytail (*Gila elegans*) and razorback sucker (*Xyrauchen texanus*). One important study limitation was that warmer inflow water temper-

atures into Lake Mead from upstream releases from Glen Canyon dam were not considered in this study, and only historic inflow temperatures were assumed. Current conditions in Lake Powell, the reservoir formed by Glen Canyon Dam, are now also at historic low surface elevations, and it is probable that release temperature conditions will increase in the future. This is the focus of future modeling efforts undertaken by the authors.

3.4.2. Time Series Results

Rising air temperatures projected by the most pessimistic climate scenario show changes to lake stratification patterns during the summer months. At LVB 6.7, loss of WSEL and volume cause the sampling site to be shallower and more susceptible to solar radiation, which causes an increase in water temperature and more pronounced warming from the baseline to the most pessimistic scenario correlating with a loss of volume in the lake (**Table 3**; Supplemental Materials SF1). Similarly, at the Hoover Dam Lower Outlet, loss of WSEL and volume causes the outlet to move closer to the surface, leading to outflow from higher in the water column where water is more vulnerable to seasonal water temperature fluctuations (**Table 5**; Supplemental Materials SF3). At CR 346.4, the largest increase in water temperature between the baseline and most pessimistic climate scenarios occurs at the highest WSEL (1100 ft (335 m)) due to heat retention by the lake in the winter and Autumn.

At CR 346.4, rising air temperature causes low DO events in winter at higher lake elevations (WSELs of 335 and 320 meters (1100 and 1050 feet); **Table 4**; Supplemental Materials SF2b). At all three sampling sites, there is also a significant trend of decreasing mean DO between the baseline and most pessimistic climate scenarios. The projected reduction is potentially impactful as two critically endangered species—the razorback sucker and bonytail—live either in Lake Mead or downstream. Harm to these or other species could occur with DO decreases. Consequently, lake managers should continue to monitor not only DO but also endangered aquatic life and prepare to adapt lake management plans as needed.

TP in Lake Mead appears nearly unchanged in this study, which is unsurprising as Lake Mead is historically phosphorus limited (LaBounty & Burns, 2005). The increased control of phosphorus from the Las Vegas Wash by wastewater treatment plants is effective in keeping TP loading to Lake Mead low, even considering lake drawdown and climate scenarios. Simulations indicate that at current discharge rates and above, TP concentrations are not expected be problematic as a result of not only drawdown but also climate change.

Bathymetry from the Las Vegas Wash entering Lake Mead is highly variable and explains the anomalous TIN concentrations at the 305 meter (1000 foot) WSEL. The depth of the sampling site LWLVB 1.2 the 305 meter (1000 foot) elevation has a shallower depth than is typically observed, measuring 17 - 21 meters. At other WSELs, the same sampling site has a depth of 26 - 30 meters. It is this change in lake bathymetry, leading to less volume for dilution for TIN en-

tering Boulder Basin, that explains the small but significant increase in TIN at the 305 meter (1000 foot) WSEL. Therefore, these larger TIN readings at 305 meters (1000 feet) are an artifact of the sampling location and complicated lake bathymetry, and not thought to be a function of significant changes in the lake's nutrient assimilation capacity.

TIN is mostly unaffected by changes in WSEL, apart from the 305 meter (1000 foot) simulation, where the sampling site moves to a shelf and a small but significant increase in TIN is observed. This increase is projected to be a consequence of lake bathymetry and sampling protocol, not degradation of water quality. Communication between wastewater dischargers and Nevada Division of Environmental Protection is recommended to alter sampling protocols around this anomalous event, so that samples can be collected and analyzed that better represent ambient water quality.

4. Conclusion

The effects of both loss of volume and projected rising air temperature on Lake Mead, a large managed reservoir in the American southwest, were studied. Five WSELs, ranging from 335 - 274 meters (900 - 1100 feet), plus air temperature increases projected by the RCP 4.5 and RCP 8.5 climate scenarios, were simulated using the LMM. These potential future scenarios illuminate probable changes to water quality and aquatic life in Lake Mead. There are six important findings from this study:

1) Nutrients (TP and TIN) are not projected to cause degradation to water quality as a result of loss of lake volume and rising air temperatures under current management practices. It is important that nutrient removal from water entering the Wash continues, as higher nutrient concentrations entering Lake Mead coupled with drawdown could have deleterious effects.

2) Water temperature is projected to increase significantly in all studied scenarios as a resulting of rising air temperatures projected by the most pessimistic climate scenario.

3) Winter and Autumn retention of heat in Lake Mead is more pronounced at higher WSELs, and the combination of the most pessimistic climate scenarios and a higher WSEL could lead to the potential for HABs.

4) Loss of volume will lead to warmer releases from Hoover Dam to downstream users.

5) DO decreases significantly as a result of rising air temperatures projected by the most pessimistic climate scenario.

6) Water temperature and DO are projected to change in ways that could impact the lake ecosystem and its aquatic life, and recreational opportunities.

This study is novel as it provides a view of how highly-managed, arid reservoirs will be affected by rising air temperatures and extreme loss of volume. These coming changes are now better understood, and management strategies to mitigate deleterious effects are provided when available. While useful, this study

does have some limitations, including utilizing historic inflow and outflow volumes and water temperatures and historic meteorological conditions. Future directions for this project include simulating the effects of drawdown in upstream reservoirs on Lake Mead and studying how changes to other meteorological parameters may affect water quality.

5. Recommendations

Recommended management strategies show that increasing or decreasing the WSEL of highly managed reservoirs, such as Lake Mead, can have different impacts and should align with targeted management goals. While solutions such as hypolimnetic oxygenation systems or lake mixers and circulators could potentially address reductions in DO and stronger, persistent thermal stratification, these products are not suitable for use in larger reservoirs such as Lake Mead due to size, cost, and anticipated oxygen demand. Changes to raw water quality at a drinking water intake are presented as a companion paper, and similar to results presented at the dam, epilimnetic withdrawals are shown to be problematic (Hannoun, Tietjen, & Brooks, 2021). The recommendations presented in this study can be applied to similarly managed arid reservoirs to proactively mitigate the effects of climate change and prolonged drought, which are projected to continue. While some negative water quality changes can be mitigated by increasing or decreasing the managed reservoir WSEL, the authors currently do not have any recommendations to ameliorate the significant effect of rising air temperatures on water temperature and DO in Lake Mead and similar reservoirs, with the exception of global GHG reduction (**Table 7**).

Table 7. Management strategies.

Concern	Management Response	Supporting Evidence
Warmer releases from dammed reservoir to downstream system	Increase WSEL of managed reservoir to prevent epilimnetic releases	**Table 5**
HABs caused by rising winter water temperatures	Decrease WSEL of managed reservoir to facilitate Autumn and winter cooling	**Table 3** **Figure 5**
Increased nutrient concentrations	Manage inflow nutrient concentration into reservoir	**Table 6**
Reductions in DO	No suggestion at this time	NA
Stronger, persistent thermal stratification	No suggestion at this time	NA
Degradation in raw water quality for treatment and distribution	Increase WSEL of managed reservoir to prevent epilimnetic withdrawals	(Hannoun, Tietjen, & Brooks, 2021)

Acknowledgements

The authors would like to thank SNWA for providing support for this project.

Conflicts of Interest

The authors declare no conflicts of interest regarding the publication of this paper.

References

Allan, M., Hamilton, D., & Muraoka, K. (2017). *A Coupled Hydrodynamic-Ecological Model to Test Management Options for Restoration of Lakes Onoke and Wairarapa.* University of Waikato.

Amadori, M., Giovannini, L., Toffolon, M., Piccolroaz, S., Zardi, D., Brescani, M. et al. (2021). Multi-Scale Evaluation of a 3D Lake Model Forced by an Atmospheric Model. *Environmental Modelling and Software, 139,* Article ID: 105017. https://doi.org/10.1016/j.envsoft.2021.105017

Butcher, J., Nover, D., Johnson, T., & Clark, C. (2015). Sensitivity of Lake Thermal and Mixing Dynamics to Climate Change. *Climate Change, 129,* 295-305. https://doi.org/10.1007/s10584-015-1326-1

Casamitjana, X., Serra, T., Colomer, J., Beserba, C., & Perez-Losada, J. (2003). Effects of the Water Withdrawal in the Stratification Patterns of a Reservoir. *Hydrobiologia, 504,* 21-28. https://doi.org/10.1023/B:HYDR.0000008504.61773.77

Chao, S., Lyra, A., Mourao, C., Dereczynski, C., Pilotto, I., Gomes, J. et al. (2014). Assessment of Climate Change in South America under RCP 4.5 and 8.5 Downscaling Scenarios. *American Journal of Climate Change, 3,* 512-525. https://doi.org/10.4236/ajcc.2014.35043

Chung, S., Hipsey, M., & Imberger, J. (2009). Modelling the Propagation of Turbid Density Inflows into a Stratified Lake: Daecheong Reservoir, Korea. *Environmental Modelling & Software, 24,* 1467-1482. https://doi.org/10.1016/j.envsoft.2009.05.016

Chung, S., Imberger, J., Hipsey, M., & Lee, H. (2014). The Influence of Physical and Physiological Processes on the Spatial Heterogeneity of a Microcystis Bloom in a Stratified Reservoir. *Ecological Modelling, 289,* 133-149. https://doi.org/10.1016/j.ecolmodel.2014.07.010

Colorado River Water Users Association (2021). *Bureau of Reclamation.* https://www.crwua.org/bor.html

Ding, L., Hannoun, I., List, E., & Tietjen, T. (2014). Development of a Phosphorus Budget for Lake Mead. *Lake and Reservoir Management, 30,* 143-156. https://doi.org/10.1080/10402381.2014.899656

Gao, Q., He, G., Fang, H., Bai, S., & Huang, L. (2018). Numerical Simulation of Water Age and Its Potential Effects on the Water Quality in Xiangxi Bay of Three Gorges Reservoir. *Journal of Hydrology, 566,* 484-499. https://doi.org/10.1016/j.jhydrol.2018.09.033

Gibbons, J., & Chakraborti, S. (2011). Nonparametric Statistical Inference. In M. Lovric (Ed.), *International Encyclopedia of Statistical Science* (pp. 977-979). CRC Press. https://doi.org/10.1007/978-3-642-04898-2_420

Hannoun, D., Tietjen, T., & Brooks, K. (2021). The Potential Effects of Drawdown on a Newly Constructed Drinking Water Intake: Study Case in Las Vegas, NV. *Water Utility Journal, 27,* 1-13.

Hodges, B., & Dallimore, C. (2013). *Estuary, Lake, and Coastal Ocean Model: ELCOM v2.2 Science Manual.* University of Western Australia.

Hodges, B., & Dallimore, C. (2019). *Aquatic Ecosystem Model: AEM3D v1.0 User Manual.* University of Western Australia.

Horne, A., & Goldman, C. (1994). *Limnology.* McGraw-Hill.

Kalansky, J., Sheffield, S., Cayan, D., & Pierce, D. (2018). *Climate Conditions in Clark County, NV: An Evaluation of Historic and Projected Future Climate Change Using Global Climate Models.* Water Utility Climate Alliance.

Kim, H., Lee, D., Park, C., & Kil, S. (2015). Evaluating Landslide Hazards Using RCP 4.5 and 8.5 Scenarios. *Environmental Earth Science, 73,* 1385-1400. https://doi.org/10.1007/s12665-014-3775-7

LaBounty, J., & Burns, N. (2005). Characterization of Boulder Basin, Lake Mead, Nevada-Arizona, USA—Based on Analysis of 34 Limnological Parameters. *Lake and Reservoir Management, 21,* 277-307. https://doi.org/10.1080/07438140509354435

MathWorks (2021). *lsqnonlin*. https://www.mathworks.com/help/optim/ug/lsqnonlin.html

Milly, P., & Dunne, K. (2020). Colorado River Flow Dwindles as Warming-Driven Loss of Reflective Snow Energizes Evaporation. *Science, 367,* 1252-1255. https://doi.org/10.1126/science.aay9187

Nevada Division of Environmental Protection (2003). *Evaluation of Total Maximum Daily Loads and Associated Water Quality Standards Attainment for the Las Vegas Wash, Las Vegas Bay and Lake Mead.* https://ndep.nv.gov/uploads/water-tmdl-docs/las_vegas_tmdl.pdf

NOAA (2019). *National Centers for Environmental Information: Daily Summaries Station Details: McCarran International Airport, NV, US*. https://www.ncdc.noaa.gov/cdo-web/datasets/GHCND/stations/GHCND:USW00023169/detail

NOAA (2022, May 11). *Comparative Climactic Data (CCD)*. https://www.ncei.noaa.gov/products/land-based-station/comparative-climatic-data

NREL (2020). Measurement and Instrumentation Data Center. https://midcdmz.nrel.gov/apps/sitehome.pl?site=UNLV

Pierce, D., Cayan, D., & Thrasher, B. (2014). Statistical Downscaling Using Localized Constructed Analogs (LOCA). *Journal of Hydrometeorology, 15,* 2558-2585. https://doi.org/10.1175/JHM-D-14-0082.1

Preston, A., Hannoun, I., List, E., Rackley, I., & Tietjen, T. (2014). Three-Dimensional Management Model for Lake Mead, Nevada, Part 1: Model Calibration and Validation. *Lake and Reservoir Management, 30,* 285-302. https://doi.org/10.1080/10402381.2014.927941

Saber, A., James, D., & Hannoun, I. (2020). Effects of Lake Water Level Fluctuation Due to Drought and Extreme Winter Precipitation on Winter Mixing and Water Quality on an Alpine Lake, Case Study: Lake Arrowhead, California. *Science of the Total Environment, 714,* Article ID: 136762. https://doi.org/10.1016/j.scitotenv.2020.136762

Sahoo, G., Forrest, A., Schladow, S., Reuter, J., Coats, E., & Dettinger, M. (2016). Climate Change Impacts on Lake Thermal Dynamics and Ecosystem Vulnerabilities. *Limnology Oceanography, 61,* 496-507. https://doi.org/10.1002/lno.10228

Saltelli, A., Tarantola, S., & Campolongo, F. (2000). Sensitivity Analysis as an Ingredient of Modeling. *Statistical Science, 15,* 377-395.

Southern Nevada Water Authority (2021). *Lower Colorado River Database*. https://exapps.lvvwd.com/WaterQuality/login.aspx?action=&uuid

Southern Nevada Water Authority (2022). *Water Resource Plan.*

Tennessee Valley Authority. (1972). *Heat and Mass Transfer between a Water Surface and the Atmosphere.* Water Resources Research Laboratory Report 14, Report No. 0-6803.

Tietjen, T. (2015). Drought and Water Quality in Lake Mead. *Lakeline,* 34-38.

Udall, B., & Overpeck, J. (2017). The Twenty-First Century Colorado River Hot Drought and Implications for the Future. *Water Resources Research, 53,* 2404-2418. https://doi.org/10.1002/2016WR019638

United States Bureau of Reclamation (2008). *2001 Lake Mead Sedimentation Survey.* U.S. Department of the Interior.

United States Bureau of Reclamation (2020b, December 21). *Reclamation Announces 2020 Colorado River Operating Conditions*. https://www.usbr.gov/newsroom/newsroomold/newsrelease/detail.cfm?RecordID=67383

United States Bureau of Reclamation. (2020a). *Lower Colorado Region: Archives of Daily Reservoir & River Conditions*. https://www.usbr.gov/lc/region/g4000/levels_archive.html

USGS (2020a). *National Water Information System: Diamond Creek near Peachtree Springs, AZ*. https://waterdata.usgs.gov/nwis/uv?site_no=09404208

USGS (2020b). *National Water Information System: Las Vegas Wash at Pabco Rd, Henderson, NV*. https://waterdata.usgs.gov/nwis/uv?site_no=09419700

USGS (2020c). *National Water Information System: Muddy River at Moapa, NV*. https://waterdata.usgs.gov/nwis/uv?site_no=09416000

USGS (2020d). *National Water Information System: Virgin River at Littlefield, AZ*. https://waterdata.usgs.gov/usa/nwis/uv?09415000

Woolway, R., Kraemer, B., Lenters, J. M., O'Reilly, C., & Sharma, S. (2020). Global Lake Responses to Climate Change. *Nature Reviews Earth & Environment, 1,* 388-403. https://doi.org/10.1038/s43017-020-0067-5

Woolway, R., Sharma, S., Wyhenmeyer, G., Debolskiy, A., Golub, M., & Mercado-Bettin, D. (2021). Phenological Shifts in Lake Stratification under Climate Change. *Nature Communications, 12,* Article No. 2318. https://doi.org/10.1038/s41467-021-22657-4

Zamani, B., Koch, M., & Hodges, B. (2020). Effects of Morphology in Controlling Propagation Density Currents in a Reservoir Using Uncalibrated Three-Dimensional Hydrodynamic Modeling. *Journal of Limnology, 79*. https://doi.org/10.4081/jlimnol.2020.1942

Supplemental Materials

Table S1. All completed LMM runs for climate change study.

Run #	RCP	WSEL (m (ft) above sea level)	Years
1	n/a	335 (1100)	baseline (2006-2007)
2	n/a	320 (1050)	baseline
3	n/a	305 (1000)	baseline
4	n/a	290 (950)	baseline
5	n/a	274 (900)	baseline
6	4.5	335 (1100)	2010-2039
7	4.5	320 (1050)	2010-2039
8	4.5	305 (1000)	2010-2039
9	4.5	290 (950)	2010-2039
10	4.5	274 (900)	2010-2039
11	8.5	335 (1100)	2010-2039
12	8.5	320 (1050)	2010-2039
13	8.5	305 (1000)	2010-2039
14	8.5	290 (950)	2010-2039
15	8.5	274 (900)	2010-2039
16	4.5	335 (1100)	2040-2069
17	4.5	320 (1050)	2040-2069
18	4.5	305 (1000)	2040-2069
19	4.5	290 (950)	2040-2069
20	4.5	274 (900)	2040-2069
21	8.5	335 (1100)	2040-2069
22	8.5	320 (1050)	2040-2069
23	8.5	305 (1000)	2040-2069
24	8.5	290 (950)	2040-2069
25	8.5	274 (900)	2040-2069
26	4.5	335 (1100)	2070-2099
27	4.5	320 (1050)	2070-2099
28	4.5	305 (1000)	2070-2099
29	4.5	290 (950)	2070-2099
30	4.5	274 (900)	2070-2099
31	8.5	335 (1100)	2070-2099
32	8.5	320 (1050)	2070-2099
33	8.5	305 (1000)	2070-2099
34	8.5	290 (950)	2070-2099
35	8.5	274 (900)	2070-2099

Table S2. Seasonal mean maximum/minimum temperature changes across all simulated climate scenarios and WSELs, Boulder Basin, Lake Mead. (a) Seasonal mean maximum/minimum water temperatures for 274 meter (900 foot) elevation in Boulder Basin, Lake Mead (˚C). (b) Seasonal mean maximum/minimum water temperatures for 290 meter (950 foot) elevation in Boulder Basin, Lake Mead (˚C). (c) Seasonal mean maximum/minimum water temperatures for 305 meter (1000 foot) elevation in Boulder Basin, Lake Mead (˚C). (d) Seasonal mean maximum/minimum water temperatures for 320 meter (1050 foot) elevation in Boulder Basin, Lake Mead (˚C). (e) Seasonal mean maximum/minimum water temperatures for 335 meter (1100 foot) elevation in Boulder Basin, Lake Mead (˚C).

(a)

		Near Term		Mid-Century		Late-Century		
	Baseline	**RCP 4.5**	**RCP 8.5**	**RCP 4.5**	**RCP 8.5**	**RCP 4.5**	**RCP 8.5**	**Max Increase**
DJF	13/12	13/12	13/12	13/12	14/12	13/12	**15/13**	2/1
MAM	18/13	18/13	18/13	19/13	19/13	19/13	**20/14**	2/1
JJA	27/16	27/16	27/16	27/16	28/16	28/16	**29/16**	2/0
SON	24/15	23/15	23/16	24/16	25/16	24/16	**26/16**	2/1

(b)

		Near Term		Mid-Century		Late-Century		
	Baseline	**RCP 4.5**	**RCP 8.5**	**RCP 4.5**	**RCP 8.5**	**RCP 4.5**	**RCP 8.5**	**Max Increase**
DJF	13/12	13/12	13/12	13/12	14/12	13/12	**15/13**	2/1
MAM	18/13	18/12	18/13	19/13	19/13	19/13	**20/13**	2/0
JJA	27/16	27/15	27/16	28/16	28/16	28/16	**29/16**	2/0
SON	23/15	23/15	23/15	24/15	24/16	24/15	**25/16**	2/1

(c)

		Near Term		Mid-Century		Late-Century		
	Baseline	**RCP 4.5**	**RCP 8.5**	**RCP 4.5**	**RCP 8.5**	**RCP 4.5**	**RCP 8.5**	**Max Increase**
DJF	13/12	13/12	13/12	13/12	14/12	14/12	**15/13**	2/1
MAM	18/13	18/13	18/13	19/13	19/13	19/13	**21/13**	2/0
JJA	27/15	27/15	27/15	28/16	28/16	28/16	**29/16**	2/0
SON	23/15	23/15	23/15	24/15	24/15	24/15	**26/16**	2/1

(d)

		Near Term		Mid-Century		Late-Century		
	Baseline	**RCP 4.5**	**RCP 8.5**	**RCP 4.5**	**RCP 8.5**	**RCP 4.5**	**RCP 8.5**	**Max Increase**
DJF	14/13	14/13	14/13	14/13	15/13	15/13	**16/14**	2/1
MAM	18/13	18/13	18/13	19/13	19/13	19/13	**20/14**	2/1
JJA	27/16	27/16	27/16	28/16	28/17	28/17	**29/18**	2/2
SON	25/16	25/16	25/16	25/16	26/17	26/17	**27/18**	2/2

(e)

	Near Term		Mid-Century		Late-Century		
	Baseline	**RCP 4.5**	**RCP 8.5**	**RCP 4.5**	**RCP 8.5**	**RCP 4.5**	**RCP 8.5**	**Max Increase**
DJF	15/13	15/13	15/13	15/14	16/14	15/14	**17/15**	2/2
MAM	18/13	18/13	18/13	19/14	19/13	19/14	**21/15**	2/2
JJA	27/16	27/16	27/16	28/17	28/17	28/17	**29/18**	2/2
SON	25/17	24/17	25/17	25/17	26/18	26/18	**27/18**	2/1

Supplemental Figures

Contour Plots at LVB 6.7, CR 346.4, and Hoover Dam.

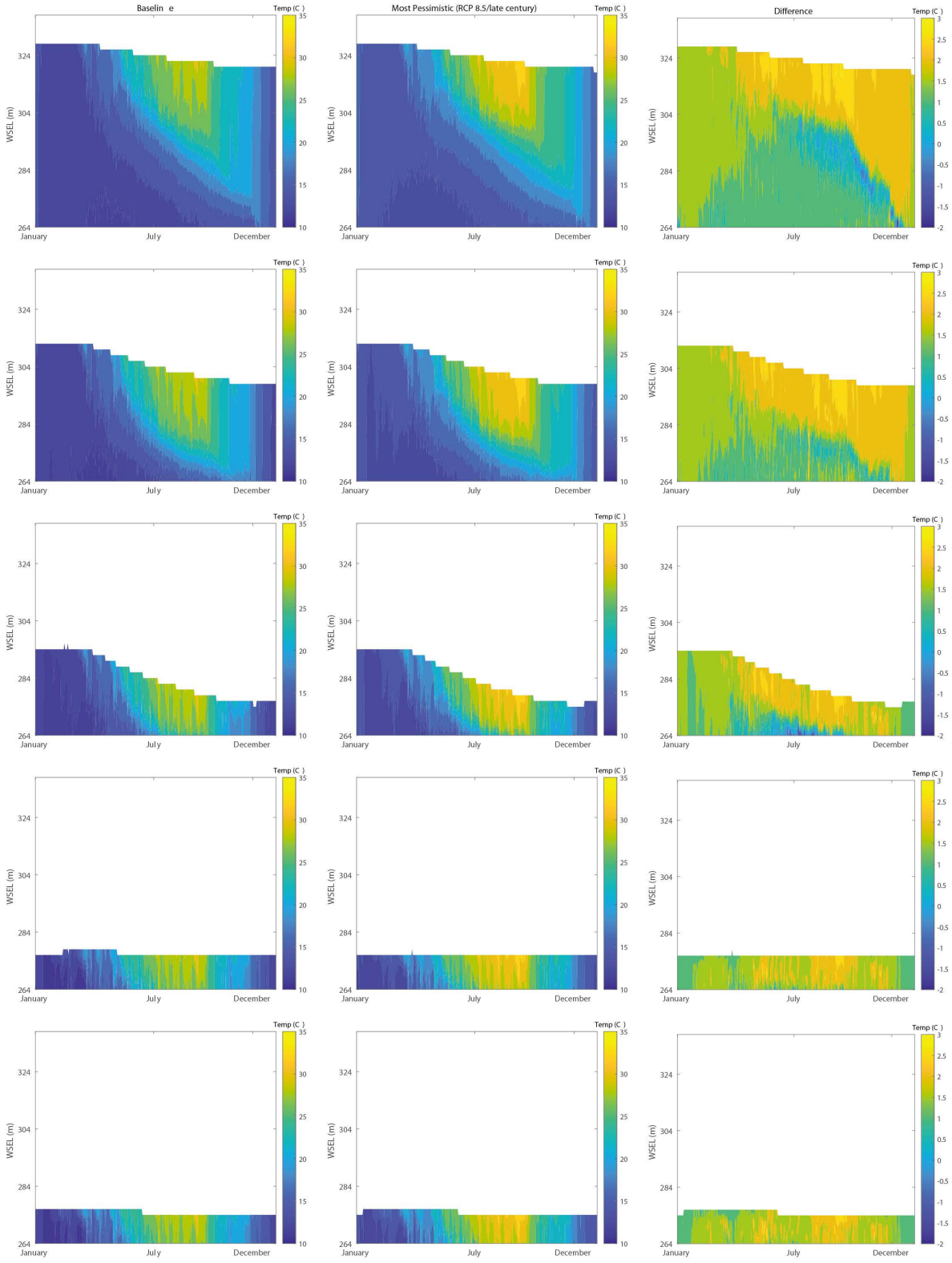

(a)

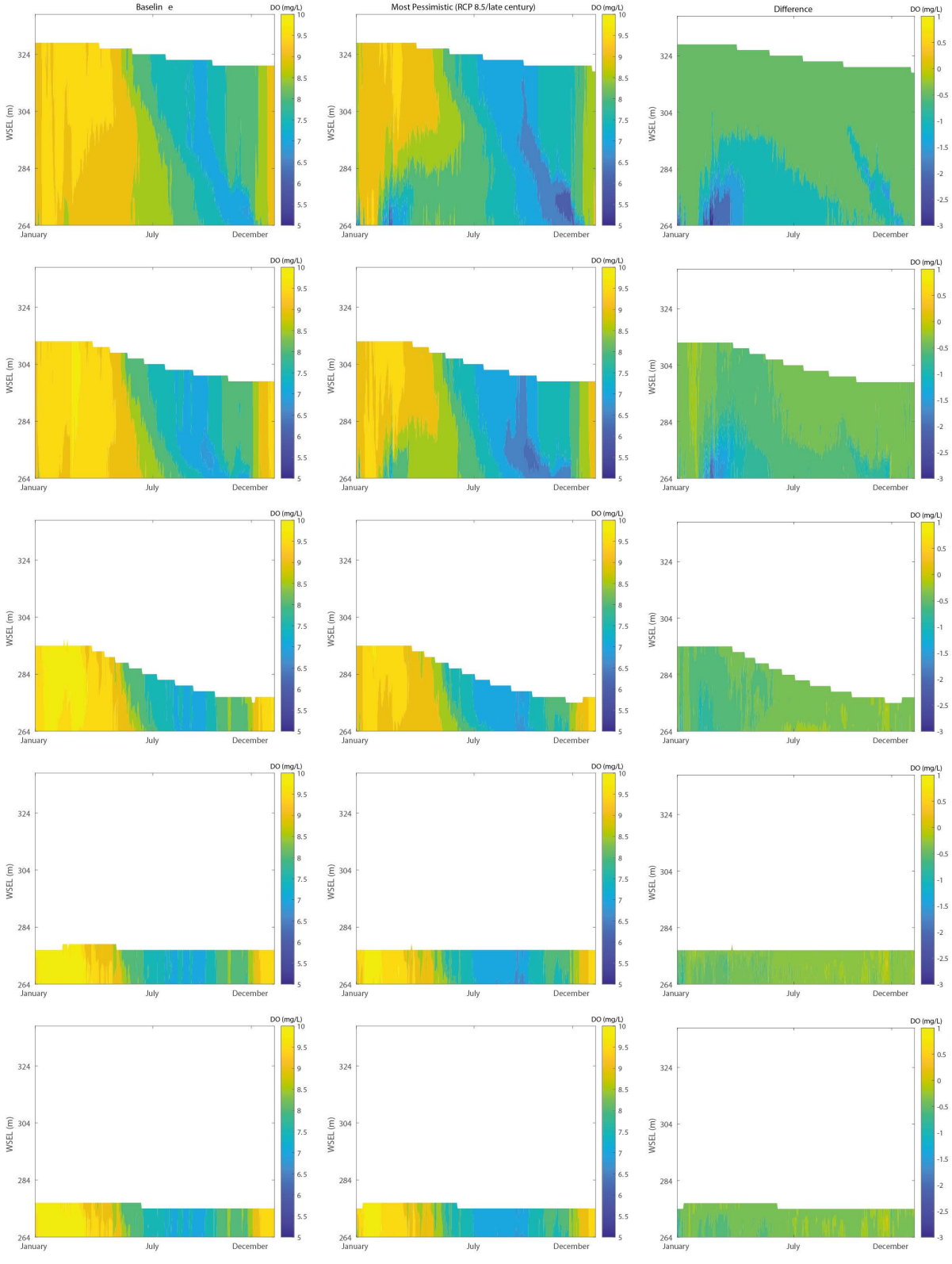

(b)

Figure S1. Water temperature and DO changes with climate impacts and lake drawdown at LVB 6.7. (a) Water temperature—baseline scenario (left); most pessimistic scenario (center); temperature difference (right). (b) DO—baseline scenario (left); most pessimistic scenario (center); concentration difference (right).

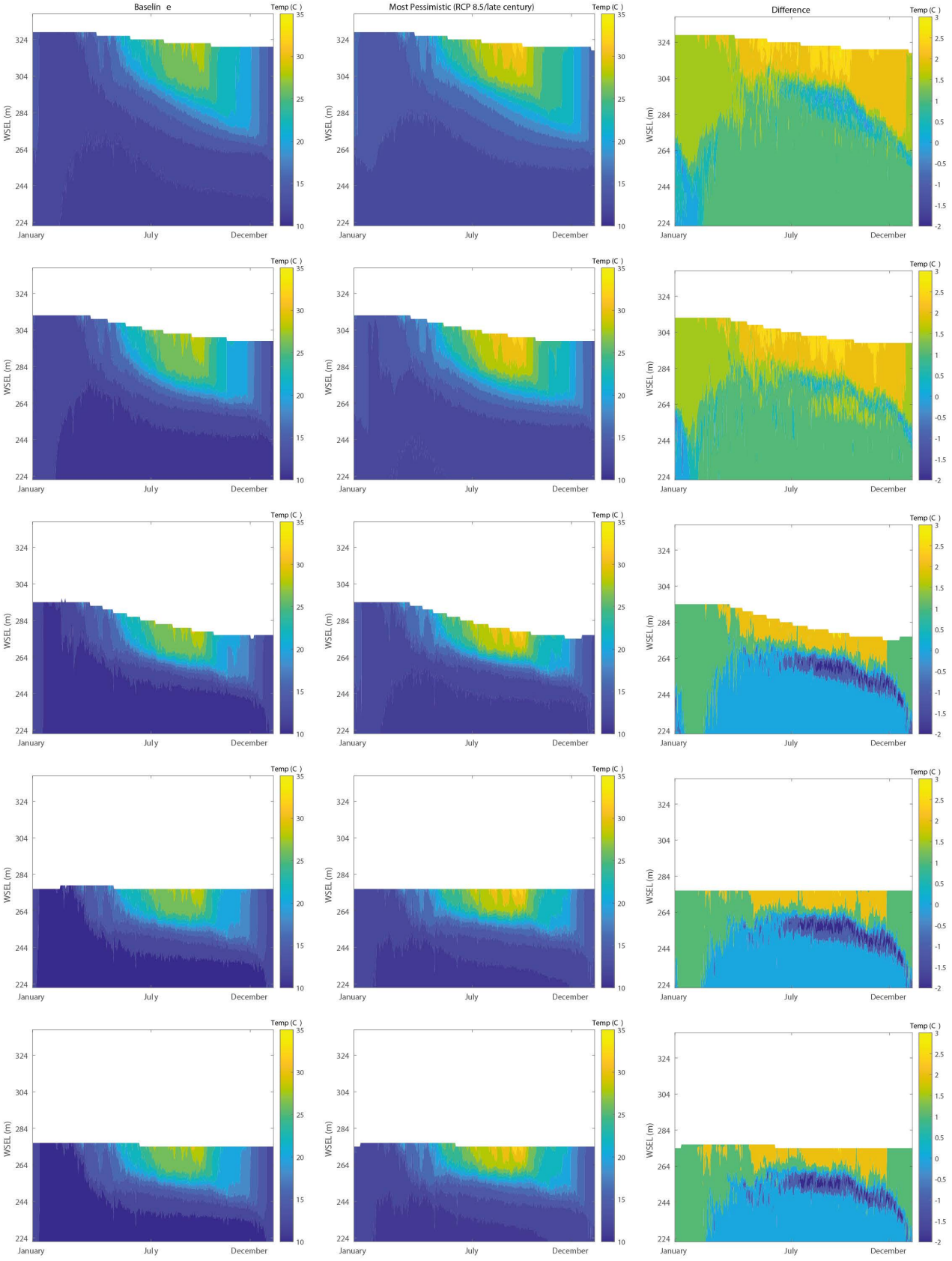
Baselin e
Most Pessimistic (RCP 8.5/late century)
Difference
Temp (C)
WSEL (m)
January
July
December

(a)

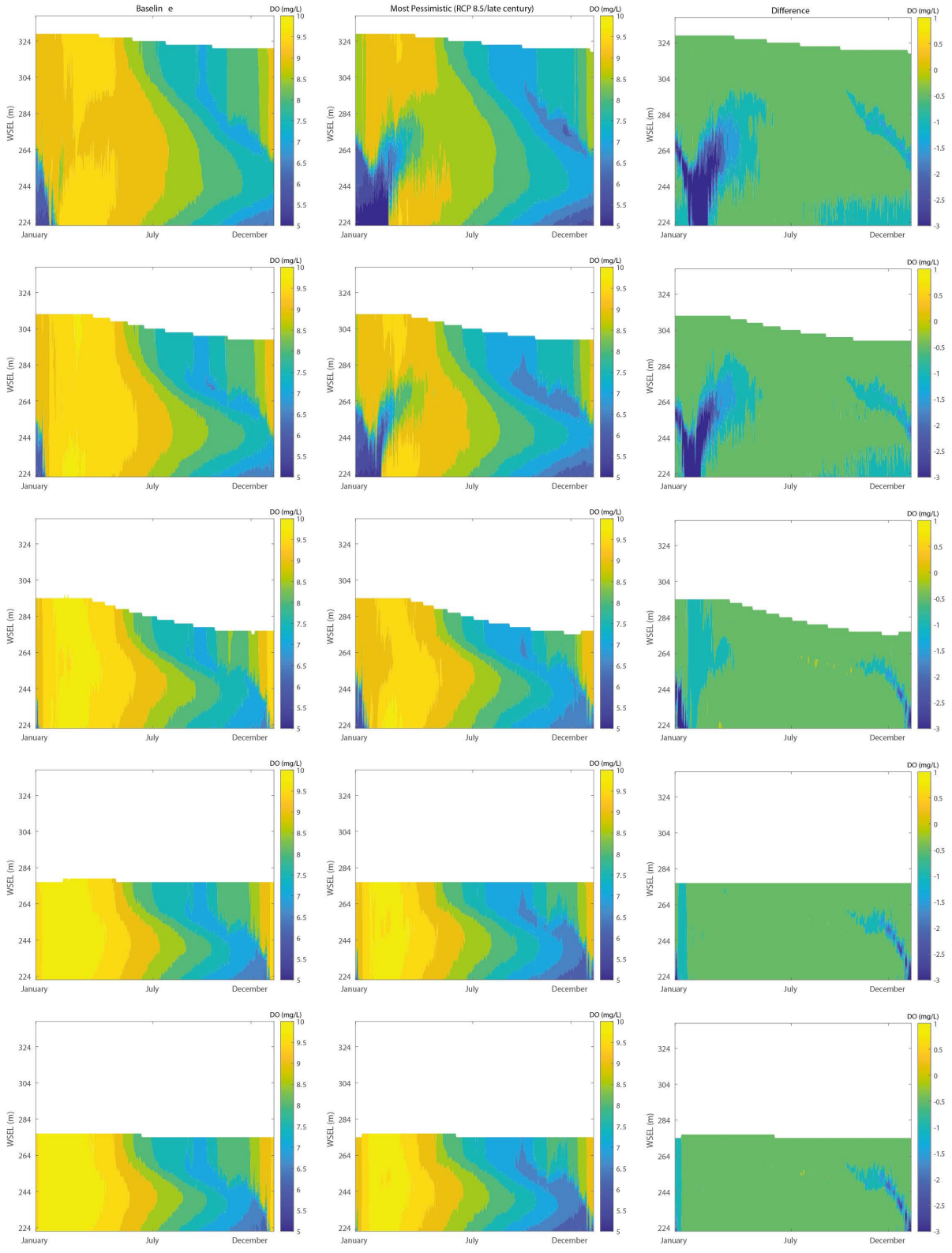

(b)

Figure S2. Water temperature and DO changes with climate impacts and lake drawdown at CR 346.4. (a) Water temperature—baseline scenario (left); most pessimistic scenario (center); temperature difference (right). (b) DO—baseline scenario (left); most pessimistic scenario (center); concentration difference (right).

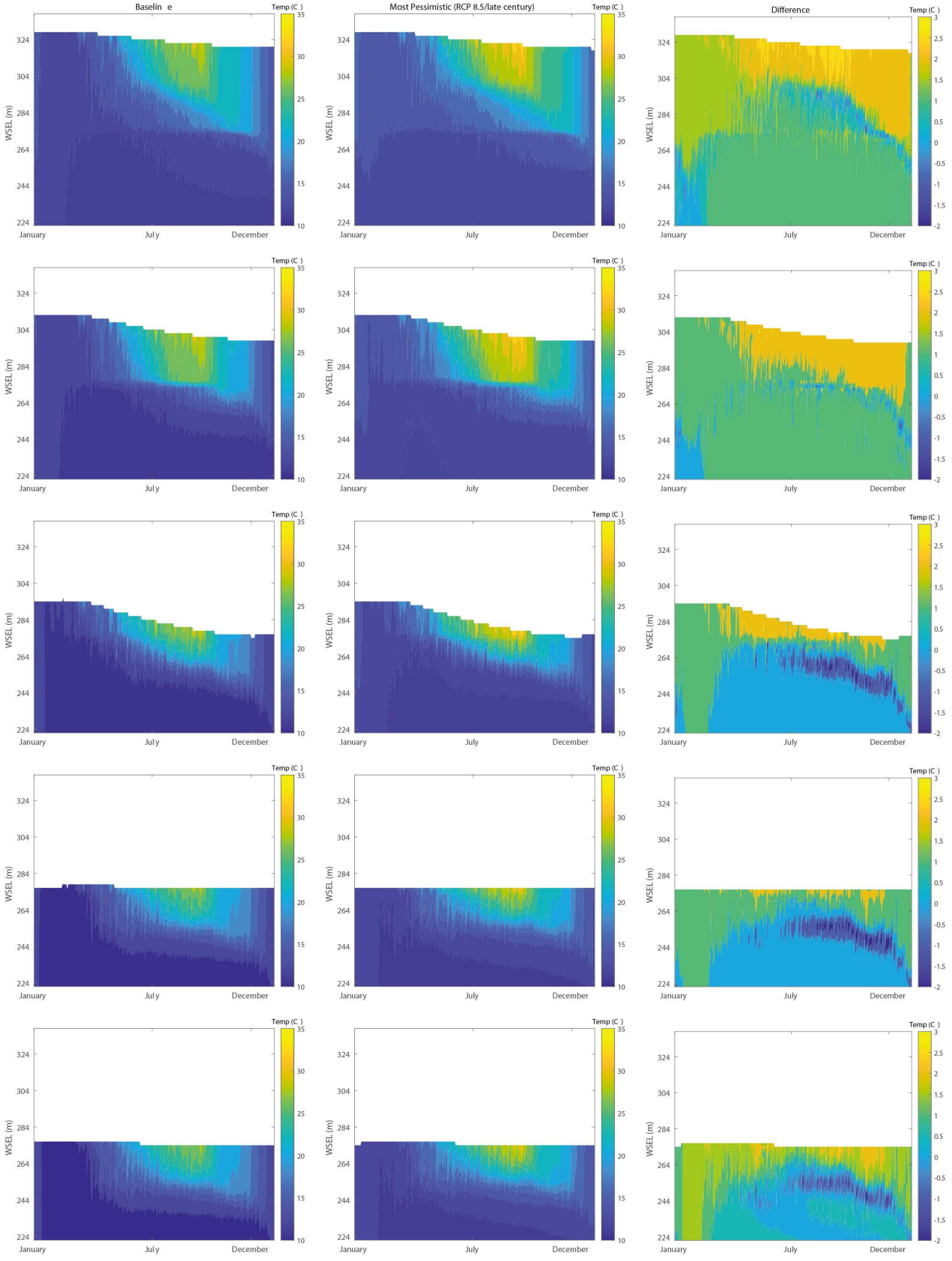
Baselin e
Most Pessimistic (RCP 8.5/late century)
Difference
Temp (C)
WSEL (m)
January
July
December

(a)

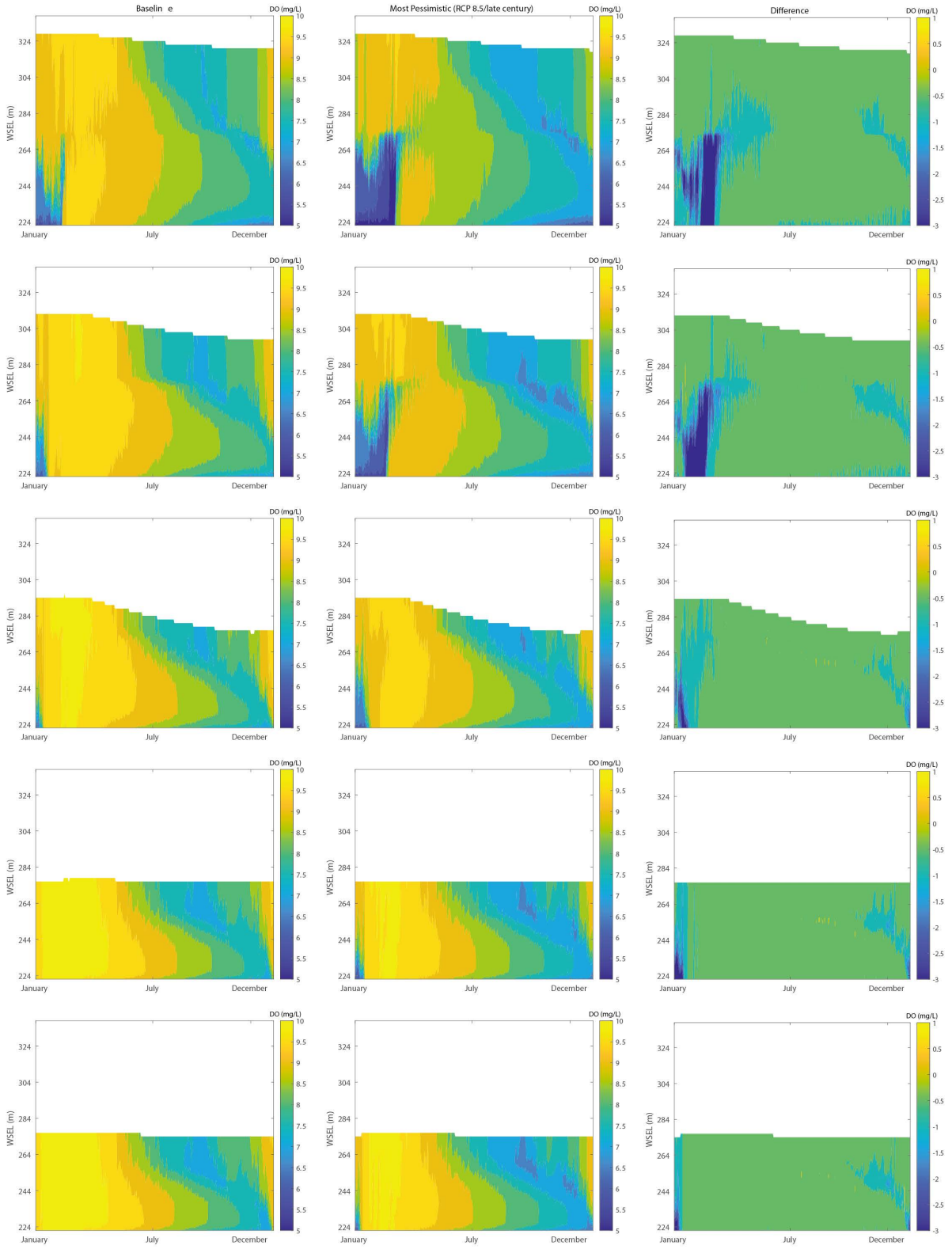

(b)

Figure S3. Water temperature and DO changes with climate impacts and lake drawdown at Hoover Dam. (a) Water temperature—baseline scenario (left); most pessimistic scenario (center); temperature difference (right). b) DO—baseline scenario (left); most pessimistic scenario (center); concentration difference (right).